3738–3745 *Nucleic Acids Research, 2008, Vol. 36, No. 11* *Published online 15 May 2008*
doi:10.1093/nar/gkn266

Fundamental differences in the equilibrium considerations for siRNA and antisense oligodeoxynucleotide design

Zhi John Lu[1] and David H. Mathews[1,2,*]

[1]Department of Biochemistry and Biophysics and [2]Department of Biostatistics & Computational Biology, University of Rochester Medical Center, Box 712, 601 Elmwood Avenue, Rochester, NY 14642, USA

Received February 22, 2008; Revised April 11, 2008; Accepted April 21, 2008

ABSTRACT

Both siRNA and antisense oligodeoxynucleotides (ODNs) inhibit the expression of a complementary gene. In this study, fundamental differences in the considerations for RNA interference and antisense ODNs are reported. In siRNA and antisense ODN databases, positive correlations are observed between the cost to open the mRNA target self-structure and the stability of the duplex to be formed, meaning the sites along the mRNA target with highest potential to form strong duplexes with antisense strands also have the greatest tendency to be involved in pre-existing structure. Efficient siRNA have less stable siRNA–target duplex stability than inefficient siRNA, but the opposite is true for antisense ODNs. It is, therefore, more difficult to avoid target self-structure in antisense ODN design. Self-structure stabilities of oligonucleotide and target correlate to the silencing efficacy of siRNA. Oligonucleotide self-structure correlations to efficacy of antisense ODNs, conversely, are insignificant. Furthermore, self-structure in the target appears to correlate with antisense ODN efficacy, but such that more effective antisense ODNs appear to target mRNA regions with greater self-structure. Therefore, different criteria are suggested for the design of efficient siRNA and antisense ODNs and the design of antisense ODNs is more challenging.

INTRODUCTION

Antisense oligonucleotides, such as siRNA or antisense oligodeoxynucleotides (ODNs), can silence gene expression (1). siRNA associate with the protein–RNA complex called the RNA-induced silencing complex (RISC) to cleave the target mRNA or attenuate the gene expression with the RNAi pathway (2–4). Antisense ODNs also bind to a complementary region of the target mRNA and generally inhibit expression by stimulating degradation of the mRNA via RNase H (5–7).

The silencing efficacies of RNAi and antisense ODNs are found to correlate with their sequence features. Efficient siRNA have preference for low G/C content, A at position 3, U at position 10, absence of G at position 13, absence of G or C at position 19, etc. (8–14). Antisense ODN silencing efficacy also correlates highly with some specific motifs of oligonucleotide sequence, such as CCAC and ACTG (15,16). Additionally, the local secondary structure of the target mRNA also influences the binding affinity of siRNA (17–20) and antisense ODNs (21–24).

In this study, predicted free energy changes of hybridization of both antisense ODNs and siRNA are compared to inhibition efficacy databases to demonstrate contrasts in the hybridization terms that influence efficacy. Free energy changes of hybridization of the antisense oligonucleotide to the mRNA target are calculated using the OligoWalk algorithm (25,26), which uses the equilibrium shown in Figure 1. The equilibrium includes self-structure terms, $\Delta G^{\circ}_{\text{intraoligonucleotide}}$, $\Delta G^{\circ}_{\text{interoligonucleotide}}$ and $\Delta G^{\circ}_{\text{target structure}}$, which correspond to the free energy change of opening intramolecular pairs in the oligonucleotide, intermolecular pairs in the oligonucleotide and base pairs in the hybridization region of the target, respectively.

The stability of duplex hybridization between antisense sequence and target is found, for the first time, to be significantly correlated with the stability of the target mRNA's self-structure at the hybridization region for both siRNA and antisense ODNs. Duplex stability is also shown to be correlated with the oligonucleotide self-structure stability for both siRNA and antisense ODNs. Different preferences of duplex stability, however, are observed for siRNA and antisense ODNs. Because RNAi is attenuated by the unwinding cost of opening the siRNA duplex, efficient siRNA (or miRNA) usually have less stable sense–antisense duplexes (27). This is just the opposite for efficient antisense ODNs, where tight

*To whom correspondence should be addressed. Tel: +01 585 275 1734; Fax: +01 585 275 6007; Email: david_mathews@urmc.rochester.edu

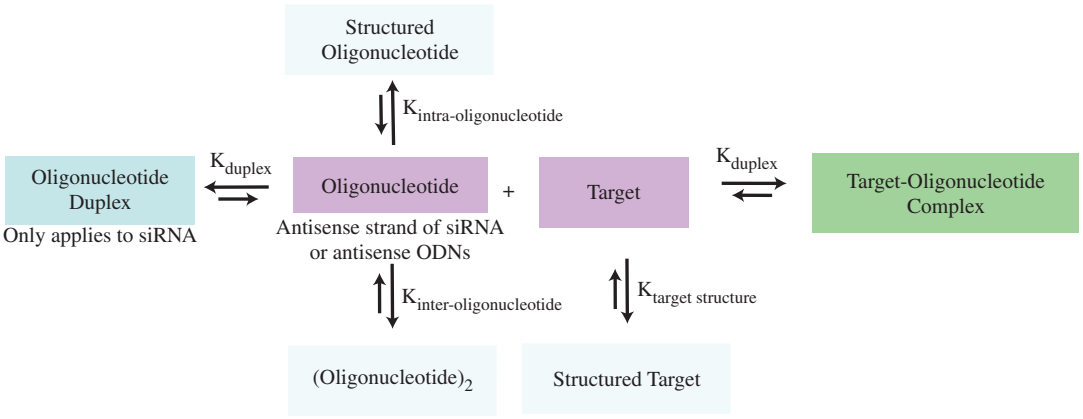

Figure 1. Equilibrium considered in the OligoWalk algorithm (25,26) for siRNA and antisense ODNs. The equilibrium constants, K_{duplex}, $K_{target\ structure}$, $K_{intraoligonucleotide}$, and $K_{interoligonucleotide}$ are related to $\Delta G^{\circ}_{duplex}$, $\Delta G^{\circ}_{target\ structure}$, $\Delta G^{\circ}_{intraoligonucleotide}$, and $\Delta G^{\circ}_{interoligonucleotide}$ by $\Delta G^{\circ} = -RT \ln K$, respectively. Self-folding in the target and self-structure in the oligonucleotide both compete with the formation of the oligonucleotide–target complex. Only RNA secondary structure interactions are considered in the calculations. The longer arrow for each equilibrium shows the generally favored direction of the equilibrium, i.e. a negative folding free energy change is predicted for an equilibrium favoring the direction of the longer arrow.

hybridization to the target is apparently required. Furthermore, in addition to duplex stability, siRNA silencing efficacy also significantly correlates with other terms such as the self-structure stabilities of siRNA and target mRNA. These correlations are not as strong for antisense ODN efficacy.

MATERIALS AND METHODS

Prediction of self-structure of oligonucleotide and target

To quantify the accessibility of oligonucleotide and target mRNA for hybridization, a free energy change of self-structure is predicted for opening base pairs in the region of complementarity to the target. A partition function (Q) calculation (28,29) is used to predict the ensemble free energy change (26). For example, the free energy cost of opening the self-structure of a target binding site is calculated using:

$$\Delta G^{\circ}_{target\ structure} = -RT \ln\left(\frac{Q_{unconstrained}}{Q_{constrained}}\right)$$

where Q is a partition function that sums the equilibrium constants for all possible structures, s.

$$Q = \sum_{s} e^{-\Delta G(s)/RT}$$

R is gas constant, T is absolute temperature, which was set to 310.15 K in this study, $Q_{unconstrained}$ is the partition function of the native target structures, $Q_{constrained}$ is the partition function of the target structures in the state where the oligonucleotide is able to bind. To predict the constrained partition function, the calculation is performed with a constraint that nucleotides in the binding region are forced single stranded. In order to reduce calculation time, $\Delta G^{\circ}_{target\ structure}$ is calculated with a partition function of the local structure on mRNA binding site, i.e. only a certain number of nucleotides centered at the binding region (800 nt) is folded (26). It was previously demonstrated that local folding of 800 nt does not significantly affect the accuracy of the accessibility prediction (26). If the binding site is located close to the 5′ or 3′ end of the target, the same size of region is folded beginning from the end of the sequence, which means the binding site is not centered on the folding region.

For the oligonucleotide, all self-structure must be broken during duplex formation with the target, so the self-structure free energy change is predicted with:

$$\Delta G^{\circ}_{oligonucleotide\ self\ structure} = -RT \ln(Q)$$

Both unimolecular and bimolecular self structure are considered for the oligonucleotide using appropriate partition functions (26).

Thermodynamic parameters

Folding free energy changes for individual structures are predicted using nearest-neighbor models. For RNA structures, the nearest neighbor parameters from Turner and co-workers are used (30). For DNA structures, the nearest neighbor parameters for DNA from the RNAstructure program (30) are used. In the case of ODN hybridization to RNA targets, DNA–RNA duplex parameters are used for helix formation (31).

Databases

The experimental data for gene silencing efficacy of oligonucleotides is derived from two databases. One is derived from an antisense ODN database, AOBase (32). 418 ODNs targeting 28 mRNA are used for this study. Thirty ODNs were removed from the original database because these sequences are not consistent in sequence with the Genbank database (33). The silencing efficacy of each oligonucleotide is represented as ln(A), the natural logarithm of Activity, which is defined as the ratio of gene expression after antisense silencing over the untreated control. For the correlation calculations, any value of activity that is <0 is reset to 0.1% and any value that

Table 1. Correlations between ln(A)[a] and free energy change terms for both siRNA and Antisense ODNs

	siRNA		Antisense ODNs	
	r	t–test P-value[c]	r	t-test P-value[c]
$\ln(A) - \Delta G^{\circ}_{duplex}$	**−0.250**	$\mathbf{1.78 \times 10^{-15}}$	**0.160**	**0.001**
$\ln(A) - \Delta G^{\circ}_{target\ structure}$[b]	**−0.197**	$\mathbf{1.11 \times 10^{-15}}$	**0.141** (0.0798)[d]	**0.004** (0.284)[d]
$\ln(A) - \Delta G^{\circ}_{intra-oligonucleotide}$	**−0.186**	$\mathbf{1.55 \times 10^{-15}}$	−0.0653 **(−0.212)**[d]	0.183 $\mathbf{(7.59 \times 10^{-7})}$[d]
$\ln(A) - \Delta G^{\circ}_{inter-oligonucleotide}$	**−0.199**	$\mathbf{3.33 \times 10^{-15}}$	−0.0467 **(−0.186)**[d]	0.341 $\mathbf{(1.45 \times 10^{-4})}$[d]
$\ln(A) - \Delta\Delta G^{\circ}_{ends}$	**−0.351**	$\mathbf{2.66 \times 10^{-15}}$	0.0587	0.231
$\Delta G^{\circ}_{duplex} - \Delta G^{\circ}_{target\ structure}$	**0.595**	$\mathbf{2.22 \times 10^{-16}}$	**0.510**	$\mathbf{4.44 \times 10^{-16}}$
$\Delta G^{\circ}_{duplex} - \Delta G^{\circ}_{intra-oligonucleotide}$	**0.524**	$\mathbf{2.22 \times 10^{-16}}$	**0.103**	**0.035**
$\Delta G^{\circ}_{duplex} - \Delta G^{\circ}_{inter-oligonucleotide}$	**0.560**	$\mathbf{<10^{-30}}$	**0.264**	$\mathbf{4.48 \times 10^{-8}}$
$\Delta G^{\circ}_{duplex} - \Delta\Delta G^{\circ}_{ends}$	0.0176	0.384	−0.0494	0.314

The correlations were calculated within Novartis data set (34) for siRNA and AOBase data set for antisense ODNs (32). r is the correlation coefficient. The definition of each free energy term is provided in the Introduction and in Figure 1.

[a]ln(A) is the natural logarithm of Activity, which is the fraction of the targeted mRNA expression after gene silencing compared to the control. Negative correlations indicate that decreasing each folding free energy change (increased stability) results in increased ln(Activity) (decreased silencing efficacy).

[b]The values were calculated with the partition function method with folding size as 800 nucleotides centered on the binding site.

[c]A P-value (probability) below 0.05 is statistically significant (significant values are shown in bold).

[d]The value in the parenthesis is the correlation coefficient for the oligonucleotides having $\Delta G^{\circ}_{duplex} \leq -30$ kcal/mol.

is >100% is reset to 99.9%. Two hundred and fifteen antisense ODNs induced more than 50% gene silencing (silencing efficacy = 1 − Activity), 103 induced more than 70% and 30 induced more than 90%. The second database is an siRNA database of experiments from Huesken *et al*. (34) at Novartis, which contains efficacy data for 2431 siRNAs targeting 31 mRNA sequences on random positions. Two thousand siRNAs have silencing efficacy >50%, 1222 of them have efficacy >70%, 369 have efficacy >90%. The silencing efficacies reported in the siRNA database are transformed to Activity (Activity = 1 − silencing efficacy) in order to calculate ln(A).

Statistical analysis

Linear correlation coefficients (r) are calculated between the free energy changes of duplex formation and free energy changes for self-structure formation in both oligonucleotide and target mRNA. Correlations are also explored between ln(Activity) and thermodynamic features involved in the equilibrium of binding for both siRNA and antisense ODNs. The significance of each linear correlation (Table 1) is tested with a two-tailed t-test. The t-test is performed with the Statistics-Basic-0.42 Perl module downloaded from: http://www.cpan.org and the data analysis tool in Excel 2004 (Microsoft Inc). For this study, a P-value of the test <0.05 is considered to be a significant correlation, i.e. rejection of the null hypothesis that the correlation is by chance.

RESULTS

The OligoWalk algorithm (25,26) was developed to predict the affinity of a structured oligonucleotide to a structured RNA target using the equilibrium shown in Figure 1. The prediction explicitly considers self-structure of the oligonucleotide and target, quantified by free energy changes calculated with the nearest neighbor model (30,31,35). The formation of self-structure ($\Delta G^{\circ}_{intraoligonucleotide}$, $\Delta G^{\circ}_{interoligonucleotide}$ and $\Delta G^{\circ}_{target\ structure}$) competes with the hybridization of the antisense oligonucleotide to the target, which is driven by the favorable free energy change of duplex formation ($\Delta G^{\circ}_{duplex}$). In addition, the stability difference between the duplex's two ends (ΔG°_{ends}) was also calculated because it is well known that efficient siRNA prefer a less stable duplex at the 5′ end of the antisense strand (8).

Duplex stability requirements are different for siRNA and antisense ODNs

In RNAi, the siRNA duplex needs to unwind for loading the antisense strand on RISC and the antisense–target duplex needs to unwind for multiple turnover. Therefore, a general rule of siRNA design is a requirement for a low G/C content in the oligonucleotide (12). It was also reported that sense–antisense duplexes of efficient siRNA (or miRNA) are less stable than inefficient siRNA in previous studies (27,36). In this study, the same trend was observed in the Novartis siRNA database (34) (Figure 2A). The average $\Delta G^{\circ}_{duplex}$ (-33.0 ± 4.6 kcal/mol) of efficient siRNA (silencing efficacy is not <70%) is 2.8 kcal/mol more than the average $\Delta G^{\circ}_{duplex}$ (-35.8 ± 5.7 kcal/mol) of inefficient siRNA (silencing efficacy is <50%). Antisense ODNs, however, do not have to destabilize the duplex formation to be efficient and, in contrast to siRNA, require stable binding to the target (Figure 2B). The difference between the average $\Delta G^{\circ}_{duplex}$ of efficient ODNs (-26.1 ± 4.2 kcal/mol) and inefficient ODNs (-24.9 ± 5.9 kcal/mol) is −1.2 kcal/mol.

The ln(A), natural logarithm of message activity, is plotted versus duplex free energy changes ($\Delta G^{\circ}_{duplex}$) of all binding sites for siRNA and antisense ODNs, in Figure 2C and D, respectively. The correlation coefficient of $\Delta G^{\circ}_{duplex}$ and ln(A) is negative ($r = -0.250$) for siRNA, yet positive ($r = 0.160$) for antisense ODNs (Table 1).

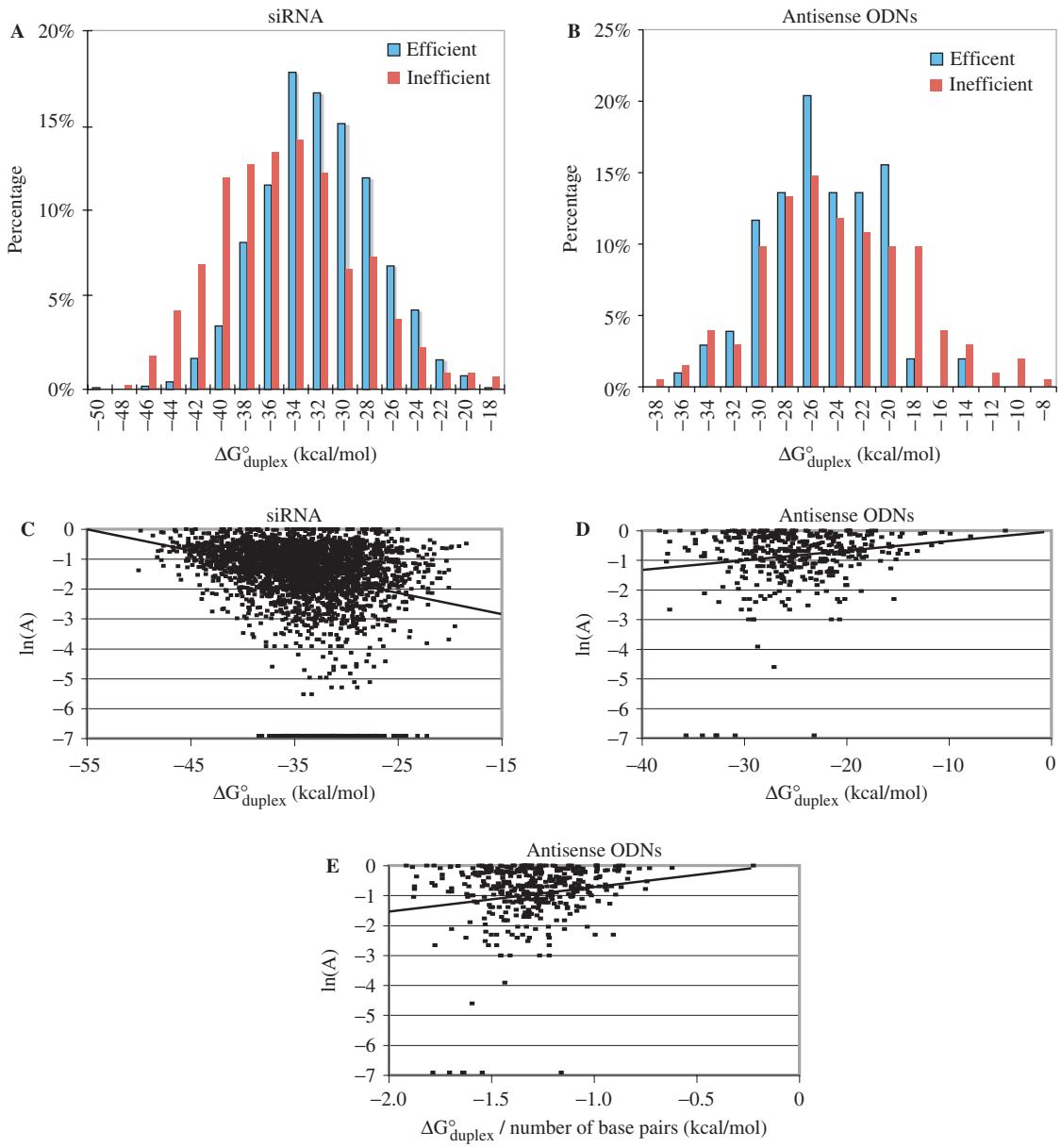

Figure 2. Oligonucleotide–target duplex stabilities in siRNA and antisense ODNs databases. The histograms of free energy changes of oligonucleotide–target duplexes ($\Delta G^{\circ}_{duplex}$) for efficient oligonucleotides (silencing efficacy is not <70%) and inefficient oligonucleotides (silencing efficacy is <50%) are shown in (**A**). the siRNA data set (34) and (**B**) the antisense ODNs data set (32). The duplex free energy change ($\Delta G^{\circ}_{duplex}$) is plotted against ln(A) for the siRNA database in (**C**) and the antisense ODNs database in (**D**). In (**E**), ln(A) is plotted as a function of the per base pair duplex free energy change for the ODNs database. ln(A) is the natural logarithm of Activity, which is the fraction of the targeted mRNA expression after antisense silencing compared to the control.

This shows again that less stable duplex formation is preferred by efficient siRNA but more stable duplexes are preferred by efficient antisense ODNs. Because the ODNs range in length from 9 to 21 nt, the correlation was also tested for ln(A) as a function of ODN duplex free energy change per base pair (Figure 2E). The correlation coefficient is 0.181, with a *P*-value of 0.000207. This is an even stronger correlation than that between ln(A) and $\Delta G^{\circ}_{duplex}$, which suggests that it is more important for antisense ODN activity to have stronger pairing per base pair than to simply favor longer helices.

Effect of self-structure appears different for siRNA and antisense ODNs

The silencing efficacy by siRNA has been previously demonstrated to be influenced by the secondary structures of both the antisense oligonucleotide and target mRNA (19,37). Each of the thermodynamic features calculated by OligoWalk, $\Delta G^{\circ}_{intraoligonucleotide}$, $\Delta G^{\circ}_{interoligonucleotide}$, $\Delta G^{\circ}_{target\ structure}$, $\Delta G^{\circ}_{duplex}$, and $\Delta\Delta G^{\circ}_{ends}$, were previously shown to correlate with the gene-silencing efficacy by siRNA (26) (Table 1).

In this study, the same terms were calculated for 418 antisense ODNs with reported inhibition activities (32,38). Significant correlations were also found between ln(A) and both $\Delta G^{\circ}_{\text{target structure}}$ and $\Delta G^{\circ}_{\text{duplex}}$ (Table 1). The correlation between ln(A) and $\Delta G^{\circ}_{\text{target structure}}$ is 0.141, which means that the more efficient antisense ODNs apparently anneal to regions of mRNA with more stable self-structure to be disrupted. This correlation is exactly opposite that for siRNAs and is counter-intuitive.

Furthermore, in contrast to siRNA, no significant correlations were observed between the free energy changes of oligonucleotide self-structure and the silencing efficacy of antisense ODNs. This is probably simply because of the wide range of ODN lengths. The correlations between oligonucleotide self-structure and ln(A) can be improved using a $\Delta G^{\circ}_{\text{duplex}}$ cutoff, where only sequences having $\Delta G^{\circ}_{\text{duplex}} \leq -30$ kcal/mol are considered. After the cutoff, the lengths of the remaining antisense ODNs vary less, as most of them have 20 or 21 nt. For this subset of antisense ODNs, the antisense efficacy is statistically significantly influenced by the self-structure of oligonucleotide (Table 1). This is consistent with previous findings for antisense ODNs (39).

In a previous study of antisense ODNs (39), the self-structure of target was poorly predicted by either optimal or suboptimal structure prediction, which are not as rigorous as the partition function calculation used here. The ambiguous correlation between antisense efficacy and $\Delta G^{\circ}_{\text{target structure}}$ in previous studies also comes from the relationship of hybridized duplex stability and self-structure accessibility of target (below).

Correlation between hybridized duplex stability and self-structure accessibility

To understand the basis of the different influence of target self-structure on siRNA and antisense ODNs, the relationship between $\Delta G^{\circ}_{\text{duplex}}$ and the self-structure folding free energy changes was explored (Figure 3A and B). It was found that the duplex free energy change correlates significantly with each of the self-structure folding free energy changes ($\Delta G^{\circ}_{\text{intraoligonucleotide}}$, $\Delta G^{\circ}_{\text{interoligonucleotide}}$ and $\Delta G^{\circ}_{\text{target structure}}$) for oligonucleotides in both the siRNA and antisense ODN database (Table 1). This correlation indicates that sequences that form stronger duplexes also tend to have stronger self-structures, both for the antisense sequences and for the target mRNA.

To control for whether this correlation is a result of a selection bias in the design of antisense sequences in the databases, it was tested for all 19mer antisense sequences in a complete scan of an mRNA (Genbank ID: X61940, length: 1933 bases) (Figure 3C). Again, the duplex-binding stability significantly correlates with the cost of opening the local self-structure of the target.

These correlations explain the apparent correlation that efficient antisense ODNs preferentially hybridize to targets with stronger self-structure. The strong correlation between target self-structure and duplex stability suggests the true preference for reduced target self-structure is obscured for ODNs because of the strong requirement for greater duplex stability. For siRNA, the correlation is readily observed because the requirement for reduced stability in the duplex also leads to a tendency for less target self-structure.

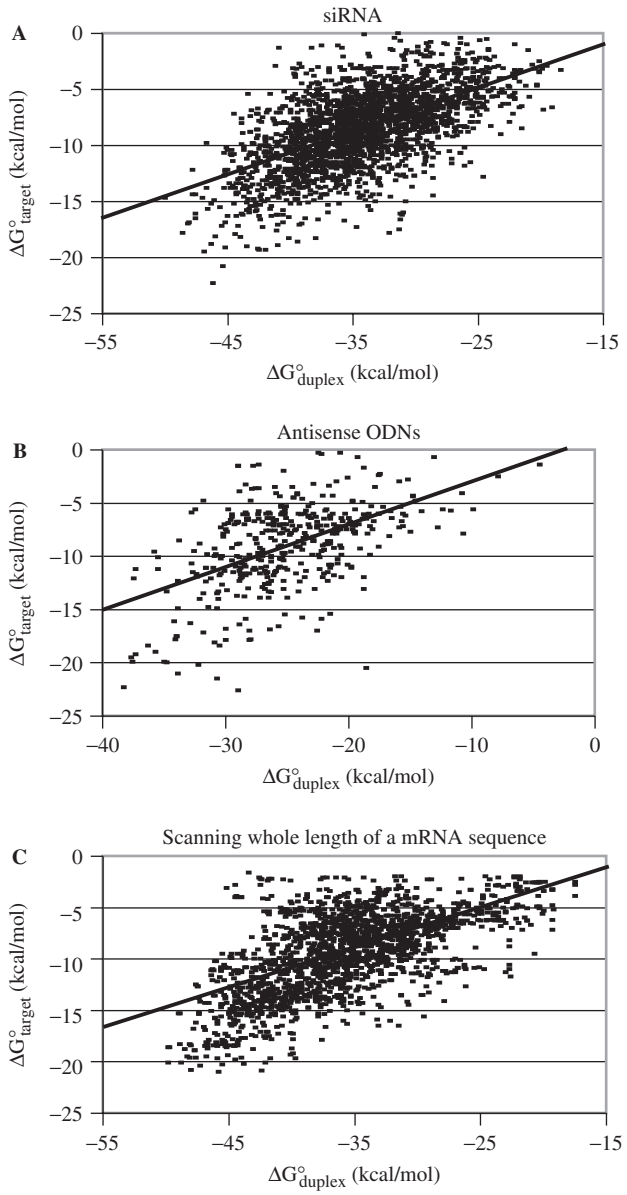

Figure 3. Correlations between free energy change of hybridized duplex ($\Delta G^{\circ}_{\text{duplex}}$) and free energy cost of opening target base pairs for hybridization ($\Delta G^{\circ}_{\text{target structure}}$). The $\Delta G^{\circ}_{\text{target structure}}$ values were calculated with a partition function with a folding size of 800 nt centered on the binding site. **(A)** For the siRNA data set (34), the correlation coefficient is 0.5946 and the *t*-test *P*-value is 2.22×10^{-16}. **(B)** For the antisense ODNs data set (32), the correlation coefficient is 0.5097 and the *t*-test *P*-value is 4.44×10^{-16}. **(C)** For a full scan of an mRNA sequence (Genbank ID: X61940, length: 1933 bases) from the 5′ end to 3′ end, the correlation coefficient is 0.6187 and the *t*-test *P*-value is 3.95×10^{-30}.

Differing equilibria for RNAi and antisense ODNs

In the initial step of RNA interference, the siRNA duplex needs to unwind (Figure 1), so the equilibrium constant

in the direction of the necessary product is $1/K_{\text{duplex}}$. Subsequently, the antisense strand hybridizes to mRNA, with the equilibrium constant for product of K_{duplex}. The cost of opening the mRNA self-tructure is $1/K_{\text{target structure}}$. The overall equilibrium, including these three effects, relates to the log of activity:

$$\ln(\text{A}) \propto K_{\text{duplex}}\left(\frac{1}{K_{\text{duplex}}}\right)\left(\frac{1}{K_{\text{target structure}}}\right)$$

Because of the positive correlation between the hybridized duplex's stability ($\Delta G^{\circ}_{\text{duplex}}$, K_{duplex}) and the target structure's accessibility ($\Delta G^{\circ}_{\text{target structure}}$, $K_{\text{target structure}}$), the proportionality is then:

$$\ln(\text{A}) \propto \frac{1}{K_{\text{target structure}}} \propto \frac{1}{K_{\text{duplex}}}.$$

This suggests that siRNA design is simple because less stable duplexes target less stable target mRNA self-structures and efficient siRNA require both of these considerations at the same time.

For antisense ODNs, however, the opposite trend emerges because there is no duplex unwinding step involved in the inhibition mechanism. The cost of opening self-structure of target and oligonucleotide competes with the formation of hybridized duplex for antisense ODNs. When the self-structure thermodynamics are compared with ln(A) for antisense ODNs, the self-structure stability correlates with the ln(A) (Table 1), but in an unintuitive manner. The hybridized duplex stability apparently accounts the most for the efficacy of antisense ODNs. Therefore, in contrast to siRNA design, the requirement of stable duplex hybridization and unstable self-structure of target simultaneously makes design difficult.

DISCUSSION

This study explores the underlying differences between the binding thermodynamics of RNAi and antisense ODNs. The preference of functional siRNA for low G/C content has been noted previously (27,40) and this leads to a lower stability for $\Delta G^{\circ}_{\text{duplex}}$ (Figure 1). It is possible that the free energy cost to unwind the siRNA is more important than the stability of oligonucleotide–target duplex. This does not apply to antisense ODNs because antisense ODNs are delivered as a single-stranded agent. Another explanation is that turnover of RISC may be facilitated by having a lower duplex affinity between the siRNA and target. The cleavage mechanism of RISC has been well studied (41–44). RISC is an endonuclease that makes a single cleavage with preference to the middle of the mRNA binding site (10 nt from the 5′ end of the siRNA) (41,45). The cleaved mRNA are released from RISC (41) and, presumably, the cleavage products are degraded in a common RNA degradation pathway because they do not have either the poly(A) tail or the 5′ cap (45,46). The antisense siRNA in RISC is then intact for another round of cleavage (46). We speculate that it is possible that RISC needs to open the base pairs between the siRNA and target mRNA strand in order to release the siRNA and RISC before degradation of the mRNA. This would lead to a preference for reduced binding strength by siRNA.

In contrast, functional antisense ODNs are known to prefer a stronger duplex affinity. In the antisense mechanism, RNase H binds to an RNA–DNA duplex and degrades the RNA. Although RNase H belongs to a nucleotidyl-transferase super family of enzymes that includes RISC (47), it may have a different process of cleavage. Experimental evidence suggests that RNase H degrades the RNA of a hybrid DNA–RNA duplex in a processive manner (48). The entire portion of the RNA strand in complex with the antisense ODN is probably degraded by RNase H and release of antisense ODN is facilitated regardless of the strength of antisense–target duplexes. Therefore, a propensity for strong duplex formation is important because it would favor target binding.

A number of studies have addressed the rational design of siRNA (12,34,49) and antisense ODNs (16,39,50), but these studies did not consider the structure features involved in the antisense binding using our rigorous partition function method. It has been demonstrated that including self-structure terms of siRNA and target mRNA helps the selection of efficient siRNA (26). The correlations found in this study show that different thermodynamic features could also be considered to improve the design of antisense ODNs. Contributions from multiple features of antisense ODNs need to be considered in order to find an optimized combination for an efficient candidate.

Another important factor in design of effective oligonucleotides is the accessibility of the target self-structure, which competes with the hybridization of the oligonucleotide to the target. The paradox demonstrated here is that the sequence features conducive to a stronger formation duplex also contribute to less binding accessibility because of self-structure of the target. This is observed as the positive correlation between the free energy changes of duplex formation and self-structure. Because siRNA favors less stable duplexes, it is easy to simultaneously avoid target structure in siRNA design. For antisense ODNs design, however, it is difficult to design strong duplexes that will bind to regions with little self-structure. This means it is fundamentally more difficult to design antisense ODNs than siRNA.

ACKNOWLEDGEMENTS

This work was supported by National Institutes of Health grant R01GM076485 to D.H.M. D.H.M. is an Alfred P. Sloan Foundation Research Fellow. The authors thank Professor Douglas H. Turner from the Department of Chemistry, University of Rochester, for discussions. The authors also thank two anonymous reviewers for constructive comments. Funding to pay the Open Access publication charges for this article was provided by the National Institutes of Health.

Conflict of interest statement. None declared.

REFERENCES

1. Scherer,L.J. and Rossi,J.J. (2003) Approaches for the sequence-specific knockdown of mRNA. *Nat. Biotechnol.*, **21**, 1457–1465.
2. Mello,C.C. and Conte,D. Jr. (2004) Revealing the world of RNA interference. *Nature*, **431**, 338–342.
3. Filipowicz,W. (2005) RNAi: the nuts and bolts of the RISC machine. *Cell*, **122**, 17–20.
4. Ameres,S.L., Martinez,J. and Schroeder,R. (2007) Molecular basis for target RNA recognition and cleavage by human RISC. *Cell*, **130**, 101–112.
5. Dias,N. and Stein,C.A. (2002) Antisense oligonucleotides: basic concepts and mechanisms. *Mol. Cancer Ther.*, **1**, 347–355.
6. Crooke,S.T. (1999) Molecular mechanisms of action of antisense drugs. *Biochim. Biophys. Acta*, **1489**, 31–44.
7. Taylor,M.F., Wiederholt,K. and Sverdrup,F. (1999) Antisense oligonucleotides: a systematic high-throughput approach to target validation and gene function determination. *Drug Discov. Today*, **4**, 562–567.
8. Khvorova,A., Reynolds,A. and Jayasena,S.D. (2003) Functional siRNAs and miRNAs exhibit strand bias. *Cell*, **115**, 209–216.
9. Schwarz,D.S., Hutvagner,G., Du,T., Xu,Z., Aronin,N. and Zamore,P.D. (2003) Asymmetry in the assembly of the RNAi enzyme complex. *Cell*, **115**, 199–208.
10. Amarzguioui,M. and Prydz,H. (2004) An algorithm for selection of functional siRNA sequences. *Biochem. Biophys. Res. Commun.*, **316**, 1050–1058.
11. Harborth,J., Elbashir,S.M., Vandenburgh,K., Manninga,H., Scaringe,S.A., Weber,K. and Tuschl,T. (2003) Sequence, chemical, and structural variation of small interfering RNAs and short hairpin RNAs and the effect on mammalian gene silencing. *Antisense Nucleic Acid Drug Dev.*, **13**, 83–105.
12. Reynolds,A., Leake,D., Boese,Q., Scaringe,S., Marshall,W.S. and Khvorova,A. (2004) Rational siRNA design for RNA interference. *Nat. Biotechnol.*, **22**, 326–330.
13. Ui-Tei,K., Naito,Y., Takahashi,F., Haraguchi,T., Ohki-Hamazaki,H., Juni,A., Ueda,R. and Saigo,K. (2004) Guidelines for the selection of highly effective siRNA sequences for mammalian and chick RNA interference. *Nucleic Acids Res.*, **32**, 936–948.
14. Yuan,B., Latek,R., Hossbach,M., Tuschl,T. and Lewitter,F. (2004) siRNA Selection Server: an automated siRNA oligonucleotide prediction server. *Nucleic Acids Res.*, **32**, W130–W134.
15. Matveeva,O.V., Tsodikov,A.D., Giddings,M., Freier,S.M., Wyatt,J.R., Spiridonov,A.N., Shabalina,S.A., Gesteland,R.F. and Atkins,J.F. (2000) Identification of sequence motifs in oligonucleotides whose presence is correlated with antisense activity. *Nucleic Acids Res.*, **28**, 2862–2865.
16. Camps-Valls,G., Chalk,A.M., Serrano-Lopez,A.J., Martin-Guerrero,J.D. and Sonnhammer,E.L. (2004) Profiled support vector machines for antisense oligonucleotide efficacy prediction. *BMC Bioinformatics*, **5**, 135.
17. Bohula,E.A., Salisbury,A.J., Sohail,M., Playford,M.P., Riedemann,J., Southern,E.M. and Macaulay,V.M. (2003) The efficacy of small interfering RNAs targeted to the type 1 insulin-like growth factor receptor (IGF1R) is influenced by secondary structure in the IGF1R transcript. *J. Biol. Chem.*, **278**, 15991–15997.
18. Far,R.K. and Sczakiel,G. (2003) The activity of siRNA in mammalian cells is related to structural target accessibility: a comparison with antisense oligonucleotides. *Nucleic Acids Res.*, **31**, 4417–4424.
19. Schubert,S., Grunweller,A., Erdmann,V.A. and Kurreck,J. (2005) Local RNA target structure influences siRNA efficacy: systematic analysis of intentionally designed binding regions. *J. Mol. Biol.*, **348**, 883–893.
20. Westerhout,E.M. and Berkhout,B. (2007) A systematic analysis of the effect of target RNA structure on RNA interference. *Nucleic Acids Res.*, **35**, 4322–4330.
21. Vickers,T.A., Wyatt,J.R. and Freier,S.M. (2000) Effects of RNA secondary structure on cellular antisense activity. *Nucleic Acids Res.*, **28**, 1340–1347.
22. Sohail,M. and Southern,E.M. (2000) Selecting optimal antisense reagents. *Adv. Drug Deliv. Rev.*, **44**, 23–34.
23. Wagner,R.W., Matteucci,M.D., Grant,D., Huang,T. and Froehler,B.C. (1996) Potent and selective inhibition of gene expression by an antisense heptanucleotide. *Nat. Biotechnol.*, **14**, 840–844.
24. Milner,N., Mir,K.U. and Southern,E.M. (1997) Selecting effective antisense reagents on combinatorial oligonucleotide arrays. *Nat. Biotech.*, **15**, 537–541.
25. Mathews,D.H., Burkard,M.E., Freier,S.M., Wyatt,J.R. and Turner,D.H. (1999) Predicting oligonucleotide affinity to nucleic acid targets. *RNA*, **5**, 1458–1469.
26. Lu,Z.J. and Mathews,D.H. (2008) Efficient siRNA selection using hybridization thermodynamics. *Nucleic Acids Res.*, **36**, 640–647.
27. Shabalina,S.A., Spiridonov,A.N. and Ogurtsov,A.Y. (2006) Computational models with thermodynamic and composition features improve siRNA design. *BMC Bioinformatics*, **7**, 65.
28. McCaskill,J.S. (1990) The equilibrium partition function and base pair probabilities for RNA secondary structure. *Biopolymers*, **29**, 1105–1119.
29. Mathews,D.H. (2004) Using an RNA secondary structure partition function to determine confidence in base pairs predicted by free energy minimization. *RNA*, **10**, 1178–1190.
30. Mathews,D.H., Disney,M.D., Childs,J.L., Schroeder,S.J., Zuker,M. and Turner,D.H. (2004) Incorporating chemical modification constraints into a dynamic programming algorithm for prediction of RNA secondary structure. *Proc. Natl Acad. Sci. USA*, **101**, 7287–7292.
31. Sugimoto,N., Nakano,S., Katoh,M., Matsumura,A., Nakamuta,H., Ohmichi,T., Yoneyama,M. and Sasaki,M. (1995) Thermodynamic parameters to predict stability of RNA/DNA hybrid duplexes. *Biochemistry*, **34**, 11211–11216.
32. Bo,X., Lou,S., Sun,D., Shu,W., Yang,J. and Wang,S. (2006) Selection of antisense oligonucleotides based on multiple predicted target mRNA structures. *BMC Bioinformatics*, **7**, 122.
33. Benson,D.A., Karsch-Mizrachi,I., Lipman,D.J., Ostell,J. and Wheeler,D.L. (2007) GenBank. *Nucleic Acids Res.*, **35**, D21–D25.
34. Huesken,D., Lange,J., Mickanin,C., Weiler,J., Asselbergs,F., Warner,J., Meloon,B., Engel,S., Rosenberg,A., Cohen,D. *et al.* (2005) Design of a genome-wide siRNA library using an artificial neural network. *Nat. Biotechnol.*, **23**, 995–1001.
35. Xia,T., SantaLucia,J. Jr, Burkard,M.E., Kierzek,R., Schroeder,S.J., Jiao,X., Cox,C. and Turner,D.H. (1998) Thermodynamic parameters for an expanded nearest-neighbor model for formation of RNA duplexes with Watson–Crick pairs. *Biochemistry*, **37**, 14719–14735.
36. Ichihara,M., Murakumo,Y., Masuda,A., Matsuura,T., Asai,N., Jijiwa,M., Ishida,M., Shinmi,J., Yatsuya,H., Qiao,S. *et al.* (2007) Thermodynamic instability of siRNA duplex is a prerequisite for dependable prediction of siRNA activities. *Nucleic Acids Res.*, **35**, e123.
37. Heale,B.S., Soifer,H.S., Bowers,C. and Rossi,J.J. (2005) siRNA target site secondary structure predictions using local stable substructures. *Nucleic Acids Res.*, **33**, e30.
38. Bo,X., Lou,S., Sun,D., Yang,J. and Wang,S. (2006) AOBase: a database for antisense oligonucleotides selection and design. *Nucleic Acids Res.*, **34**, D664–D667.
39. Matveeva,O.V., Mathews,D.H., Tsodikov,A.D., Shabalina,S.A., Gesteland,R.F., Atkins,J.F. and Freier,S.M. (2003) Thermodynamic criteria for high hit rate antisense oligonucleotide design. *Nucleic Acids Res.*, **31**, 4989–4994.
40. Holen,T., Amarzguioui,M., Wiiger,M.T., Babaie,E. and Prydz,H. (2002) Positional effects of short interfering RNAs targeting the human coagulation trigger tissue factor. *Nucleic Acids Res.*, **30**, 1757–1766.
41. Martinez,J. and Tuschl,T. (2004) RISC is a 5′ phosphomonoester-producing RNA endonuclease. *Genes Dev.*, **18**, 975–980.
42. Rivas,F.V., Tolia,N.H., Song,J.J., Aragon,J.P., Liu,J., Hannon,G.J. and Joshua-Tor,L. (2005) Purified Argonaute2 and an siRNA form recombinant human RISC. *Nat. Struct. Mol. Biol.*, **12**, 340–349.
43. Song,J.J., Smith,S.K., Hannon,G.J. and Joshua-Tor,L. (2004) Crystal structure of Argonaute and its implications for RISC slicer activity. *Science*, **305**, 1434–1437.
44. Tolia,N.H. and Joshua-Tor,L. (2007) Slicer and the argonautes. *Nat. Chem. Biol.*, **3**, 36–43.

45. Elbashir,S.M., Martinez,J., Patkaniowska,A., Lendeckel,W. and Tuschl,T. (2001) Functional anatomy of siRNAs for mediating efficient RNAi in *Drosophila melanogaster* embryo lysate. *EMBO J.*, **20**, 6877–6888.
46. Haley,B. and Zamore,P.D. (2004) Kinetic analysis of the RNAi enzyme complex. *Nat. Struct. Mol. Biol.*, **11**, 599–606.
47. Nowotny,M., Gaidamakov,S.A., Crouch,R.J. and Yang,W. (2005) Crystal structures of RNase H bound to an RNA/DNA hybrid: substrate specificity and metal-dependent catalysis. *Cell*, **121**, 1005–1016.
48. Gaidamakov,S.A., Gorshkova,I.I., Schuck,P., Steinbach,P.J., Yamada,H., Crouch,R.J. and Cerritelli,S.M. (2005) Eukaryotic RNases H1 act processively by interactions through the duplex RNA-binding domain. *Nucleic Acids Res.*, **33**, 2166–2175.
49. Ladunga,I. (2007) More complete gene silencing by fewer siRNAs: transparent optimized design and biophysical signature. *Nucleic Acids Res.*, **35**, 433–440.
50. Far,R.K., Leppert,J., Frank,K. and Sczakiel,G. (2005) Technical improvements in the computational target search for antisense oligonucleotides. *Oligonucleotides*, **15**, 223–233.